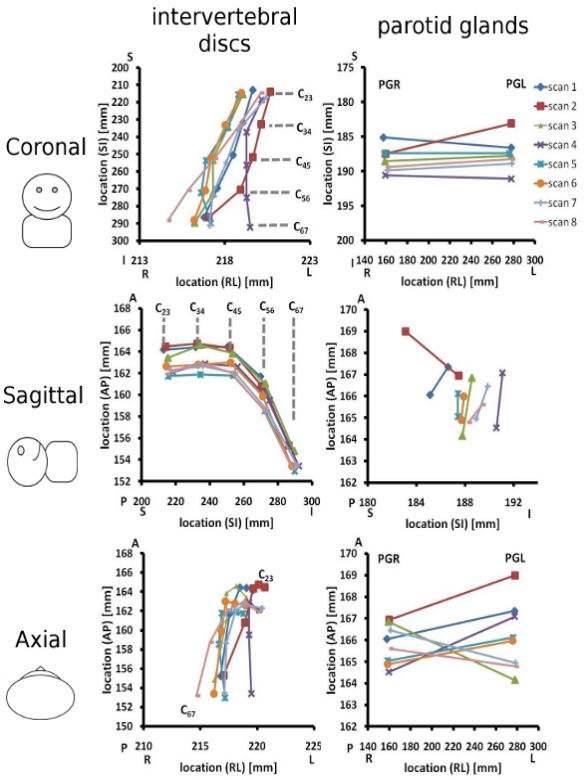

Conclusions: Our results in discs suggest that comparable positional repeatability could be achieved on MR-sim to that in real RT-treatment as previously revealed by CT. More importantly, we illustrated on MR-sim, for the first time, that organ at risk like PG could present pronounced inter-scan positional variability, suggesting the potential merit of MR-sim to visualize soft tissue for inter-fraction positional verification in head and neck radiotherapy to reduce toxicity.

PO-0971

Segmentation of organs at risk using superpixels on MRI or CT images in prostate radiotherapy

M. Guinin[1], S. Ruan[2], L. Nkhali[3], B. Dubray[3], L. Massoptier[1], I. Gardin[4]

[1]*AQUILAB, Research and Innovation, Lille, France*

[2]*University of Rouen, Litis Quantif EA4108, Rouen, France*

[3]*Henri Becquerel Center, Radiotherapy, Rouen, France*

[4]*Henri Becquerel Center, Nuclear Medicine, Rouen, France*

Purpose/Objective: Segmentation of organs at risk (OAR) in male pelvis is critical for planning prostate cancer radiotherapy. Our aim was to segment OAR of male pelvis (i.e. femoral heads, bladder and rectum) on MRI or CT images, using a 3D semi-automatic method based on a superpixel algorithm.

Materials and Methods: The initial step consists in uniformly positioning *K* seeds on the image to be segmented. These seeds are expanded over the image by aggregating similar neighboring pixels forming so-called superpixels through an Eikonal-based region growing clustering algorithm. Then, an adjacency graph is calculated from these superpixels. The user selects several superpixels belonging to each OAR to be segmented, so that the corresponding nodes in the adjacency graph are labelled. The final segmentation is obtained by carrying out a graph diffusion. The influence on segmentation results of the number (*K*) of superpixels has been assessed with Dice Indices (DI) on 7 MRI and 8 CT patients' data with respective sizes of 320×320×20 and 512×512×148 pixels. The gold standard was the segmentation performed by an experienced radiation oncologist. The intra-user reproducibility has been evaluated and our results have been compared with those previously published using other segmentation algorithms on CT (Met_1 [Thörnqvist, Acta Oncol, 2010], Met_2 [Acosta, Prostate Cancer Imaging, 2010] and Met_3 [Huyskens, Radiother & Oncol, 2009]), and MRI (Met_4 [Dowling, Prostate Cancer Imaging, 2010]).

Results: The segmentation of all OARs took about five minutes per patient. For both image modalities and the 3 OARs, the DI increased with *K* to reach a plateau at *K*=300 for MRI and *K*=500 for CT. Under these conditions, the results were DI_{MRI} = 82.3% ± 0.8% and DI_{CT} = 88.6% ± 2.8% for the femoral heads, DI_{MRI} = 60.8% ± 10% and DI_{CT} = 92.1% ± 3.3% for the bladder, and DI_{MRI} = 72.3% ± 6.6% and DI_{CT} = 73.8% ± 3.1% for the rectum. The worst results were obtained for the bladder on MRI images, since the radiation oncologist contoured the external side of the bladder wall and our method delineated the inner side. Our method gave good intra-user reproducibility results: DI on MRI and CT are 97.2% ± 1.8% and 93.1% ± 3.5% (femoral heads), 93.2% ± 5.5% and 93.2% ± 4.9% (bladder), and 86.8% ± 10.2% and 89% ± 10.2% (rectum), respectively. For MRI, our method gave better results than Met_4 using an atlas, for the segmentation of rectum, but not for segmentation of femoral heads and bladder with $DI_{MRI}(Met_4)$ values of 89.0% ± 1.0% (femoral heads), 64.0% ± 18% (bladder), and 65.0% ± 2.0% (rectum). On CT images, our method consistently yielded the best results when compared with the 3 other methods ($Met_{1,2,3}$).

Conclusions: Our method based on superpixels provides an interactive, fast and efficient segmentation of male pelvis OARs on MRI and CT. A future work will be to use the segmented bladder and rectum to automatically delineate the prostate.

Poster: Physics track: Imaging: focus on QA and technical aspects

PO-0972

Geometric verification of Dynamic Wave Arc using orthogonal X-ray fluoroscopic imaging

M. Burghelea[1], D. Verellen[1], K. Poels[1], T. Gevaert[1], T. Depuydt[1], K. Tournel[1], M. De Ridder[1], M. Hiraoka[2], V. Simon[3]

[1]*Universitair Ziekenhuis Brussel, Department for Radiation Oncology, Brussels, Belgium*

[2]*Kyoto University Graduate School of Medicine, Department of Radiation Oncology and Image-applied Therapy, Kyoto, Japan*

[3]*Babes Bolyai University, Faculty of Physics, Cluj Napoca, Romania*

Purpose/Objective: To describe an independent methodology of determining Gantry/Ring angular positions using the on-board orthogonal fluoroscopy system of the Vero machine. The method was applied to determine the

geometric accuracy of synchronized Gantry/Ring rotations during Dynamic Wave Arc deliveries, a new feature developed for the O-ring design.

Materials and Methods: The Dynamic Wave Arc (DWA) combines simultaneously Gantry/Ring (G/R) rotations, offering additional range of treatment orientations without involving patient/couch motion. Different non-coplanar wave trajectories were generated in order to investigate the influence of path complexity on delivery accuracy. A cubic phantom with five ball-bearing was used to determine the G/R positional information from fluoroscopic images acquired during DWA delivery. The detected angular positions (DetPositions) were benchmarked against the G/R angulations retrieved from the DICOM RT plan (CP), and the command log files specified by the treatment unit before delivery (LogCmd). The G/R rotational accuracy was quantified as the mean absolute deviation +/- standard deviation. The G/R maxim deviation was calculated as the maxim 3D distance between the CP and the closest DetPositions.

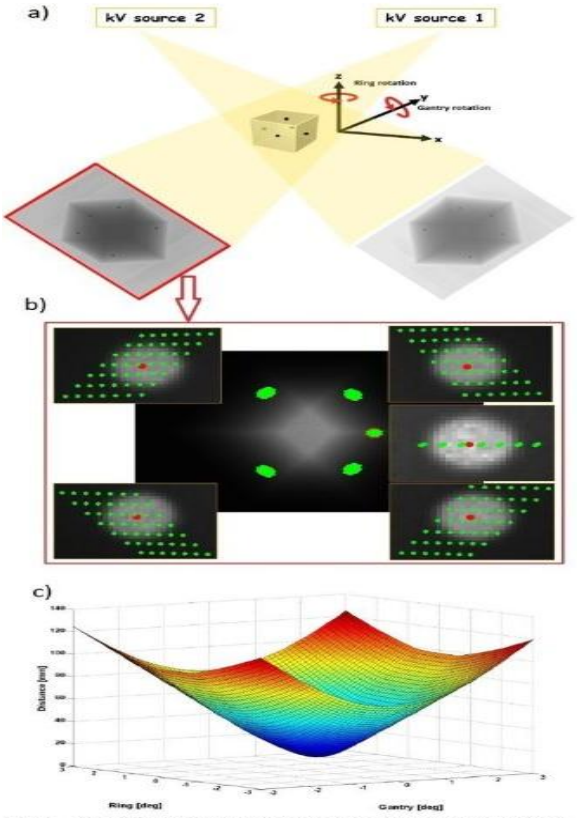

Figure An illustration of the G/R detection process for G/R=0°0°. a) Orthogonal kV images of the cubic phantom with BBs attached are acquired. b) The projected BBs positions are detected (red dots) and a set of predicted positions in the interval G±3°, R±3° is generated (green dots). c) In the search interval, the smallest distance between detected and predicted positions will provide the G/R angulation.

Results: In the CP vs. DetPositions comparison, a G/R overall mean deviation of 0.13°/0.16° ± 0.16°/0.16° was obtained with a G/R maxim of 0.6°/0.2°. For the LogCmd vs. DetPoints evaluation, the overall mean deviation was 0.07°/0.14° ± 0.09°/0.10° with a G/R maxim of 0.4°/0.4°. The largest decoupled deviations registered for Gantry and Ring were 0.6° and 0.5° respectively. No directional dependence was observed between clockwise and counter clockwise rotations. Doubling the dose resulted in a double number of detected points around each CP, and an angular deviation reduction in all cases.

Table Results from the geometric accuracy analysis performed for all Dynamic Wave Arc trajectories investigated, presented as the mean G/R absolute deviation ± SD and maxim G/R absolute deviation.

Abbreviations:

CP=Control Points, G/R angulations derived from the DICOM plan; DetPositions=Detected Positions, detected G/R angulations from the fluoroscopic images; LogCmd= Log Commanded, G/R angulations specified by the controller before delivery; SD=standard deviation.

	CP vs. DetPositions		LogCmd vs. DetPositions	
DWA trajectories	G/R mean deviation ± SD [deg]	G/R max deviation [deg]	G/R mean deviation ± SD [deg]	G/R max deviation [deg]
D1_CW	0.12°/0.20° ± 0.17°/0.09°	0.3°/0.2°	0.05°/0.21° ± 0.07°/0.08°	0.0°/0.3°
D1_CCW	0.18°/0.20° ± 0.10°/0.20°	0.4°/0.3°	0.03°/0.23° ± 0.07°/0.08°	0.0°/0.4°
D1_CW_DD	0.07°/0.16° ± 0.10°/0.07°	0.2°/0.2°	0.03°/0.19° ± 0.04°/0.07°	0.0°/0.4°
D2_CW	0.10°/0.07° ± 0.15°/0.09°	0.3°/0.1°	0.13°/0.06° ± 0.15°/0.03°	0.4°/0.0°
D2_CCW	0.11°/0.11° ± 0.11°/0.09°	0.3°/0.0°	0.16°/0.01° ± 0.10°/0.05°	0.4°/0.0°
D2_CW_DD	0.09°/0.06° ± 0.10°/0.08°	0.2°/0.1°	0.14°/0.0° ± 0.15°/0.02°	0.3°/0.2°
T1_CW	0.17°/0.13° ± 0.18°/0.14°	0.3°/0.3°	0.06°/0.17° ± 0.08°/0.05°	0.1°/0.4°
T1_CCW	0.09°/0.30° ± 0.13°/0.13°	0.1°/0.4°	0.09°/0.27° ± 0.09°/0.08°	0.0°/0.4°
T1_CW_DD	0.05°/0.21° ± 0.09°/0.17°	0.2°/0.3°	0.06°/0.16° ± 0.07°/0.14°	0.2°/0.4°
T2_breast	0.12°/0.13° ± 0.16°/0.15°	0.4°/0.1°	0.04°/0.12° ± 0.07°/0.14°	0.1°/0.3°
T3_cranial	0.24°/0.18° ± 0.30°/0.20°	0.6°/0.2°	0.09°/0.17° ± 0.11°/0.20°	0.1°/0.4°
T4_liver	0.24°/0.14° ± 0.29°/0.17°	0.6°/0.1°	0.07°/0.14° ± 0.09°/0.16°	0.0°/0.4°
T5_saw	0.12°/0.18° ± 0.17°/0.23°	0.5°/0.2°	0.02°/0.04° ± 0.10°/0.19°	0.4°/0.4°

Conclusions: The methodology described in this work can provide a simple and efficient pre-treatment verification for Vero acceptance testing or clinical Quality Assurance procedures, independent of future developments in dose optimization or trajectory optimization. The geometric verification approach was successfully applied on diverse wave paths and showed that the Vero system is capable of following complex trajectories with G/R accuracy below 0.6°±0.1°.

PO-0973

Monte Carlo study of Cone-Beam CT dose variation with patient size

K. Joshi[1], T. Marchant[1]

[1]*The Christie NHS Foundation Trust, Christie Medical Physics and Engineering, Manchester, United Kingdom*

Purpose/Objective: Modern fan beam CT scanners modulate imaging dose to account for differences in patient size. In contrast, most radiotherapy gantry based CBCT based systems offer fixed exposure imaging protocols. Dose modulation is not performed, which can result in poor quality images for larger patients, and smaller patients receiving a larger dose than necessary.

In the absence of dose modulation a solution would be to set up separate imaging protocols for patients of different sizes. We used Monte Carlo simulations to study the variation in CBCT dose with patient size. AAPM TG 204 [1] investigated